

PRESSURIZED MEMBRANES FOR STRUCTURAL USE: INTERACTION BETWEEN LOCAL EFFECTS AND GLOBAL RESPONSE

RICCARDO BARSOTTI^{*} AND SALVATORE S. LIGARÒ[†]

^{*} Department of Civil Engineering
University of Pisa
Largo L. Lazzarino, 1 56126 Pisa, Italy
e-mail: r.barsotti@ing.unipi.it

[†] Department of Civil Engineering
University of Pisa
Largo L. Lazzarino, 1 56126 Pisa, Italy
e-mail: s.ligaro@ing.unipi.it

Key words: Inflatable beams, Wrinkling, Non-linear elastic behaviour.

Summary. This paper is aimed to assess the non-linear elastic response of an inflatable cylindrical beam through a simple mechanical model recently proposed by the authors¹ to study the equilibrium shapes of highly pressurized elastic membranes. The local geometric nonlinearities due to the wrinkling of the membrane are taken into account by means of an equivalent physical non-linearity, assuming a two-states constitutive law for the material: when a fiber is stretched (the active state), its response is elastic, while when the fiber is contracted, no compressive force can be engendered in it (the passive state). The evolution of the wrinkled regions and the distribution of longitudinal and transverse stresses in the membrane are accurately determined for increasing levels of loads, up to the collapse. The numerical results, obtained through an expressly developed incremental-iterative algorithm, are then compared with the experimental ones available in the literature.

1 INTRODUCTION

In recent years the number of applications where use has been made of textile structures under form of pressurized membranes has seen a steady growth in many areas of engineering. Compared to ordinary structures, inflatable ones are lighter and economic, are easily portable, and enable their rapid set up and final removal.

Beams and arches, made of highly pressurized very flexible membranes, properly strengthened by textile or glass fibers, are a viable alternative to more traditional choices in all those cases in which the speed of execution or the lightness constitute primary requirements (consider, for example, all the emergency situations where shelters need to be erected as soon as possible, or the structures designed to operate in the space). However, some basic aspects characterizing the mechanical response of the inflatable elements have not yet entirely cleared and may therefore be placed among the current topics of mechanics of structures².

The equilibrium states of these elements are characterized by strong geometrical nonlinearities (local buckling and wrinkling phenomena) due to the smallness of membrane

thickness values, which may interest large portions of their surface. Moreover, with increasing loads, the size of the corrugated zones, whose position constitutes one of the main unknowns of the problem, tends to increase, thus strongly influencing the overall behaviour of the whole element and, what it is most important, its actual carrying capacity.

In this paper we assess the state of stress in the wall of an inflatable cylindrical beam through a simple mechanical model recently proposed by the authors to study the equilibrium shapes of highly pressurized elastic membranes¹. The aforesaid local geometric nonlinearities are taken into account by means of an equivalent physical non-linearity, assuming a two-states constitutive law for the material: when a fiber is stretched (the active state), its response is elastic, while when the fiber is contracted, no compressive force can be engendered in it (the passive state). The evolution of the corrugated regions and the distribution of longitudinal and transverse stresses in the membrane are determined accurately for increasing levels of loads, up to the collapse. The numerical results, obtained by an expressly developed incremental-iterative algorithm, are then compared with the numerical and experimental ones available in the literature^{3,4}.

2 THE BENDING OF AN INFLATABLE BEAM

In the following, we will investigate the bending response of a cylindrical inflatable beam, variously supported at its ends, subjected to a transversal concentrated load $2F$ acting in the middle section (Figure 1). The beam is made up of two rectangular elastic sheets of initial length $2L$ and height h , joined together along their common boundaries.

In all the cases examined the dimensions of the beam are kept fixed, as well as the mechanical parameters of the material. The equilibrium problem will be solved for different values of the pressure p and of the transversal load $2F$ for each of the two cases corresponding to simply-supported and built-in ends, respectively.

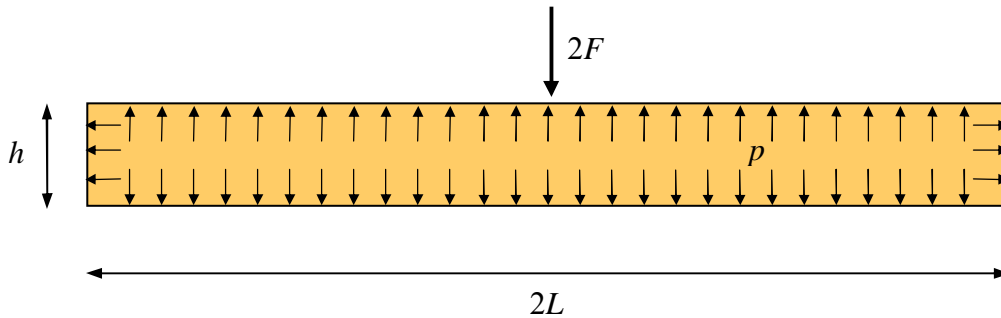


Figure 1: the inflatable beam.

The solutions will be obtained numerically by making use of an expressly developed incremental-iterative algorithm implemented in a FEM code, already proposed by the authors, which accounts for the local geometric nonlinearities resulting from the wrinkling of the membrane by means of an equivalent physical non-linearity.

To improve the rate of convergence and the stability of the numerical algorithm, the load process is subdivided into three separate phases. The membrane starts the load process in its

reference configuration where it is flat and unstressed. During the first phase, the pressure is kept equal to zero while a uniform antagonist plane traction is assumed to act along the boundary until a final value for it is reached. During the successive phase two, an increasing pressure p acts internally, up to its established final value. Finally, in the following phase three the boundary traction progressively reduces to zero and wrinkling may freely develop. In all the three phases the analysis is performed by the same incremental-iterative procedure although the first pre-tensioning phase may be performed within a single load step.

At the end of each incremental step, equilibrium is imposed via the virtual work principle. Large displacements and strains are considered, while a nonlinear elastic constitutive law which makes use of a relaxed energy is included into the analytical model to account for wrinkling.

In all the numerical analyses the membrane material is assumed to behave as linear elastic under tension with a Young's modulus of $E = 2.5$ GPa and a Poisson's ratio of $\nu = 0.3$; the membrane thickness is set equal to 0.125 mm, the height and the length of the beam are set equal to 126 mm and 660 mm, respectively.

2.1 A simply-supported beam

The first case taken under investigation is that of the simply-supported inflatable beam showed in Figure 2. It is assumed that the beam, initially lying in the x - y plane, is first inflated up to the final pressure p (accordingly, the central part of the beam becomes a cylinder of radius approximately equal to $R = 40$ mm); then, it is subjected to the action of the load $2F$. By virtue of symmetry, only one half of the beam has been modeled (Figure 3a).

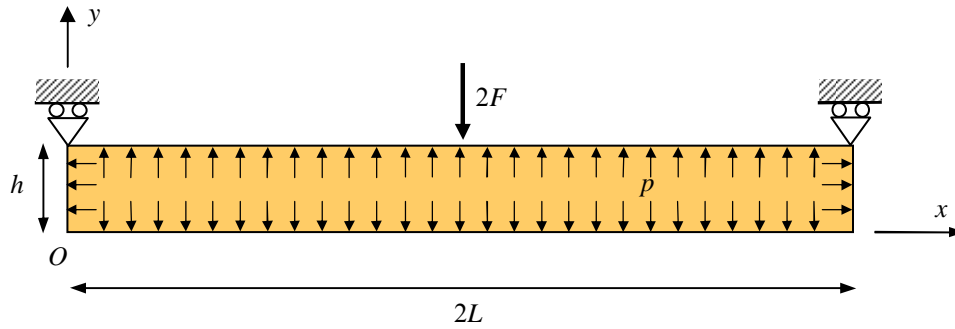


Figure 2: the simply-supported inflatable beam.

The inflated configuration together with three equilibrium configurations is showed in Figure 3. In the picture, wrinkled elements are represented in red colour, taut ones in bleu.

After the beam is inflated some first wrinkled zones appear in correspondence to the simply-supported end; in the following loading phase a second wrinkled region spreads itself in the middle of the beam as the concentrated load increases. In the case where the internal pressure is kept fixed, the wrinkled region at the end of the inflated beam turns out to be almost unaffected by the magnitude of the load F . The effects of end wrinkled regions, measured in terms of strains and stresses, are detectable only in the lateral parts of the beam¹

while the standard uniform tensile state of stress persists in the cylindrical central part of the inflated configuration (see Figure 3b).

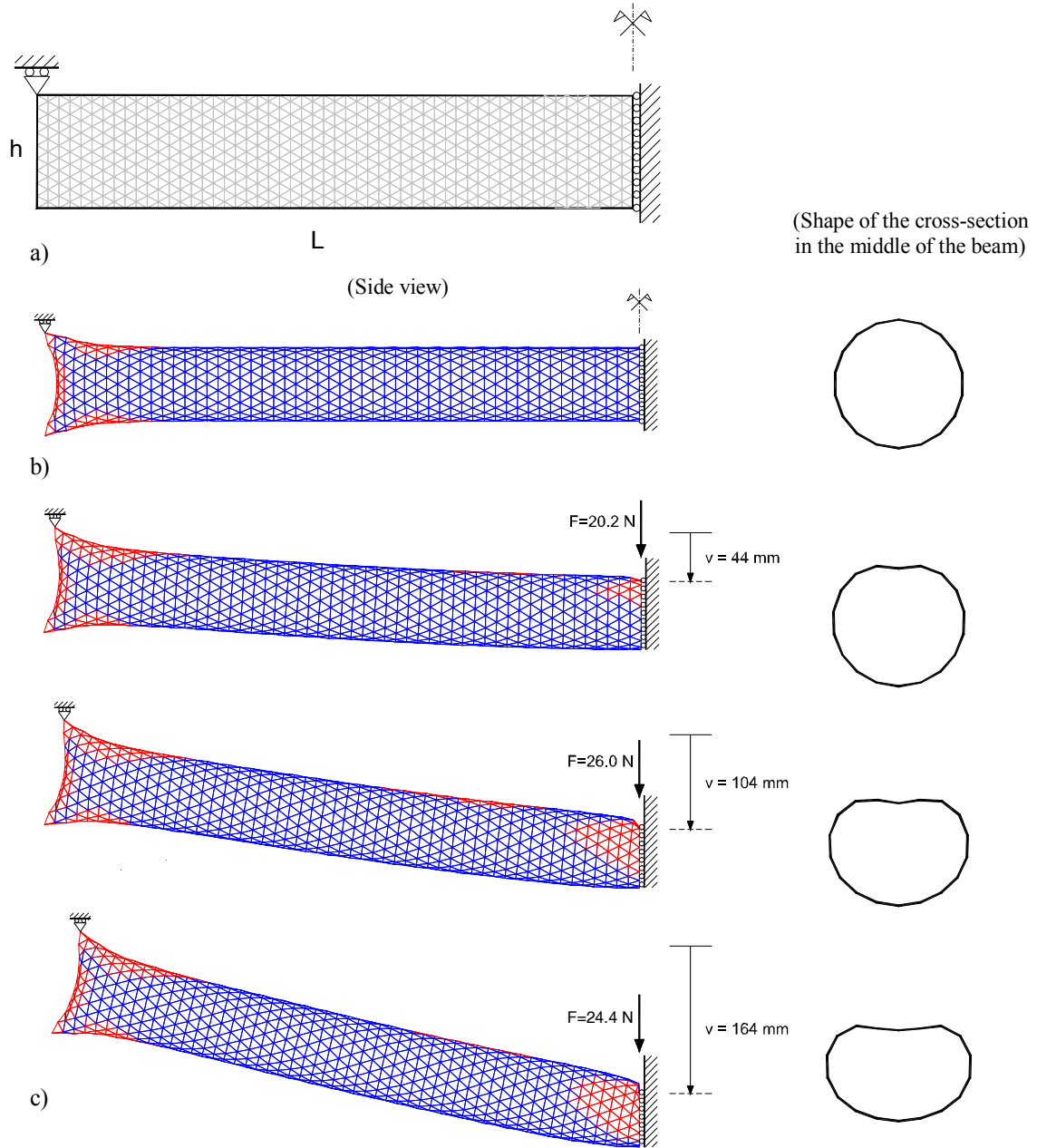


Figure 3: a) the FEM mesh; b) the inflated configuration; c) three equilibrium configurations corresponding to $F = 20.2$ N, 26.0 N and 22.4 N respectively (left half of the beam; red elements are in a wrinkled state; $p = 0.1$ N/mm², $E = 2500$ N/mm², $\nu = 0.3$, $t = 0.125$ mm)

On the contrary, the extension of the wrinkled region under the point load increases with F and the wrinkling produces effects which are not confined to a local scale but influence the load-displacement response of the inflated beam as a whole.

Figure 4 shows the central part of the beam. A noteworthy mechanical phenomenon emerges from a closer observation of the evolution of the shape of the wrinkled region under the point load. As one may easily verify, the spreading of wrinkles due to the compressive stresses produced by the bending moment (which is maximum in the middle section) is hindered by an increase in the tensile stresses at the extrados of the beam due to the local punching action of the concentrated load $2F$.

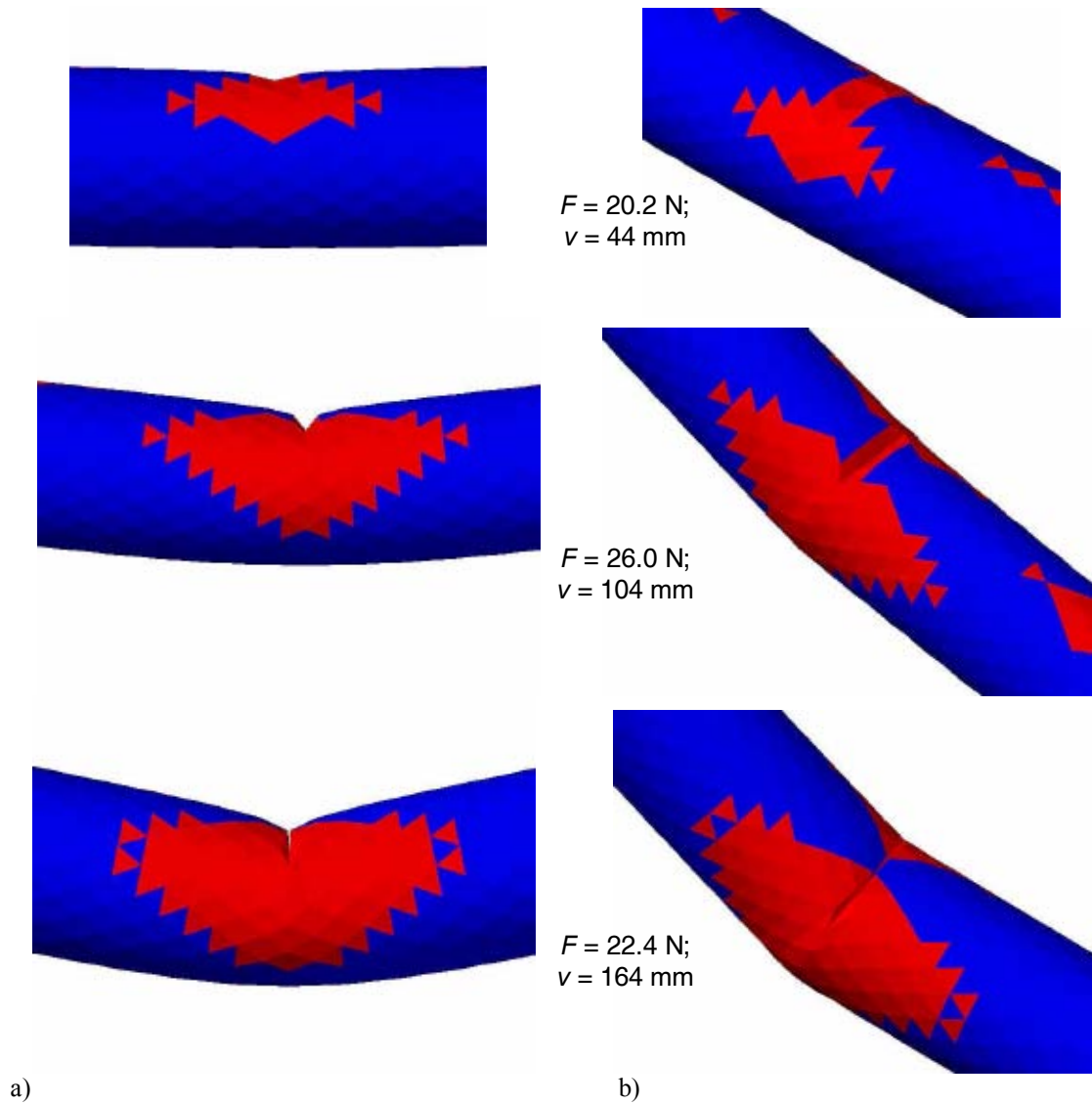


Figure 4: wrinkled region in the middle of the beam for $F = 20.2 \text{ N}$, 26.0 N and 22.4 N .
a) side view; b) axonometric view ($p = 0.1 \text{ N/mm}^2$, $E = 2500 \text{ N/mm}^2$, $\nu = 0.3$, $t = 0.125 \text{ mm}$).

As a result, the wrinkled region is smaller than that which would be forecasted by means of a one-dimensional beam model; consequently, the stiffness of the inflated beam in the three-dimensional model will be higher. Notwithstanding this, it is reasonable to think that the load-displacement response of the present 3d model would be in good agreement with that

obtained by a one-dimensional model (a confirmation of this may be found, for example, in reference²). In fact, the increase in the stiffness due to the reduction of the wrinkled region is balanced by an increase in the vertical displacements due to the local punching action of the force $2F$.

To highlight this feature two load-displacement curves, one regarding the application point of the load and the other the corresponding point on the axis of the inflatable beam, are showed in Figure 5. Both are obtained by using the present three-dimensional model in the case where the pressure p is kept fixed to the value of 0.1 N/mm^2 , the Young's modulus and the Poisson's ratio of the membrane are set equal to $E = 2,500 \text{ MPa}$ and $\nu = 0.3$, respectively, and the membrane thickness is assumed equal to $t = 0.125 \text{ mm}$.

In the same figure, a straight line starting from the origin and whose slope is the stiffness:

$$k_{el} = \frac{24E\pi R^3 t}{L^3},$$

represents the response of a standard linear elastic beam. As it can be seen, this straight line results tangent to the load-displacement curve of the inflated beam (obviously, the one regarding the displacement of the point of the line of axis in correspondence to the loaded point) within a good approximation. The tangent stiffness here obtained, equal to 0.66 N/mm , results quite close to that obtained numerically³ (0.68 N/mm) for a cantilever inflated beam having half the span of the beam considered here and the same geometrical and mechanical properties.

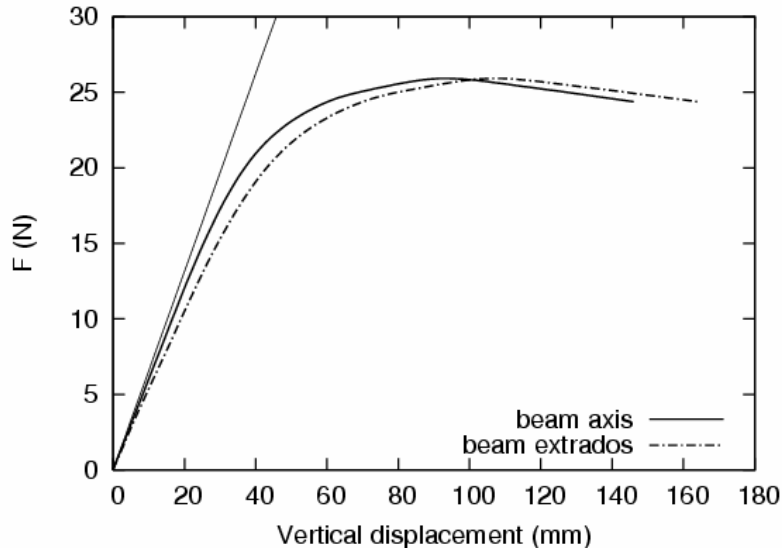


Figure 5: load-displacement curve for $p = 0.1 \text{ N/mm}^2$ ($E = 2500 \text{ N/mm}^2$, $\nu = 0.3$, $t = 0.125 \text{ mm}$).

It is worth observing that the differences between the two load-displacement curves of Figure 5 increase linearly for low values of the load, i.e. when the central part of the inflated beam is slightly wrinkled only in proximity of the loaded point. The same difference results instead to be quite constant when the load approaches its limit value and a spreading of wrinkles in the central part of the inflated beam is observed. The increase in the vertical displacement due to the punching effect may also explain the commonly observed difference

between experimental and theoretical displacements⁴.

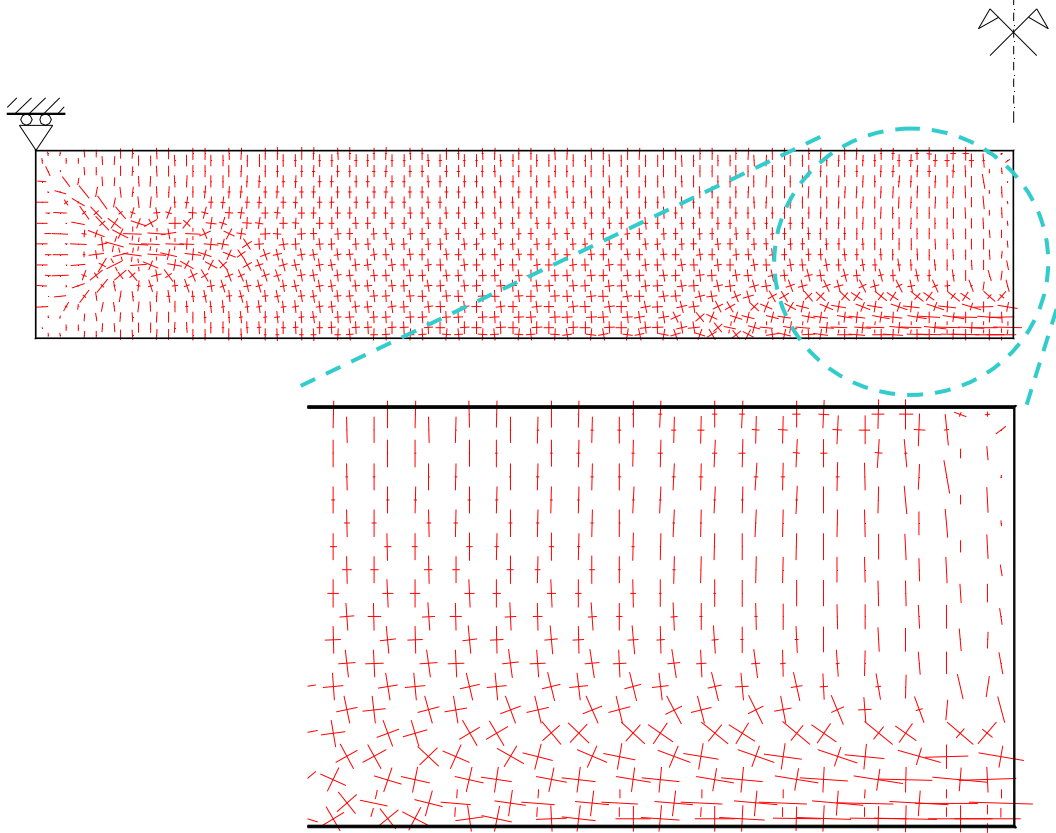


Figure 6: principal stresses in the membrane for vertical displacement of the point of application of the load equal to 164 mm (left half of the beam; $p = 0.1 \text{ N/mm}^2$, $E = 2500 \text{ N/mm}^2$, $\nu = 0.3$, $t = 0.125 \text{ mm}$).

The stress distribution in the membrane obtained by the same non-linear FEM analysis confirms the presence of the wrinkled region in the middle of the beam. Moreover, it provides with useful hints about the magnitude of the transversal stresses and about the transmission of the shear force. As an example, the case illustrated in Figure 6 clearly shows that in the central part of the beam, where a wide wrinkled region is present, the circumferential tensile stresses are far from being uniform so the shear force is transmitted almost exclusively by the unwrinkled part of the cross-section.

The stiffening effect produced by an increasing internal pressure is showed in Figure 7. Here, the load vs. pressure diagram is obtained by imposing to the loaded point a fixed displacement of 84 mm and by checking the magnitude of the load for increasing pressure. Two different responses are recognizable depending on whether the pressure is lower or higher than a threshold value, which in the case examined turns out to be equal to about 0.4 N/mm^2 . In the low pressure range ($p < 0.4 \text{ N/mm}^2$), the central part of the beam is in a wrinkled state and a small increase in the pressure results in a strong stiffening of the beam (to this regard, in Figure 7 the dashed straight line representing the separation curve between wrinkled and unwrinkled responses of the beam is plotted). For higher pressures instead ($p > 0.4 \text{ N/mm}^2$), the beam is unwrinkled and the stiffening effect is due to the decrease in the

displacements in the small punched region just under the load.

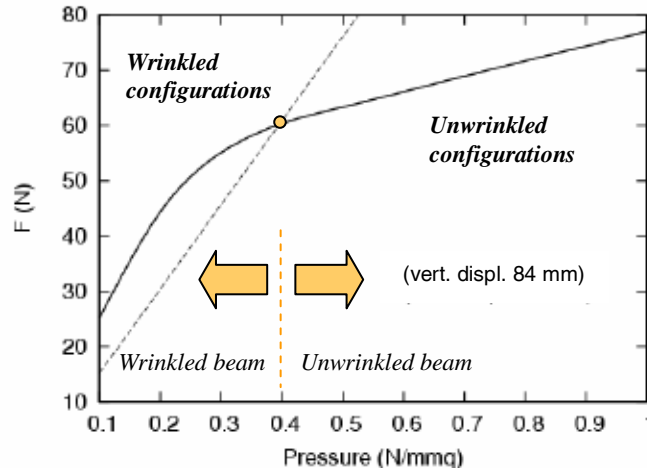


Figure 7: load vs. pressure diagram for vertical displacement of the loaded point equal to 84 mm ($p = 0.1 \text{ N/mm}^2$, $E = 2500 \text{ N/mm}^2$, $\nu = 0.3$, $t = 0.125 \text{ mm}$).

2.2 The built-in beam

The second case taken under consideration is that of the built-in inflatable beam showed in Figure 8. It is assumed that the built-in constraint is first imposed to both the ends of the beam, which initially lies in the x - y plane. Then the beam is inflated up to the final pressure p (accordingly, the central part of the beam becomes a cylinder of radius approximately equal to $R = 40 \text{ mm}$) and finally the load $2F$ is applied. Once again, by virtue of symmetry, only one half of the beam has been modeled.

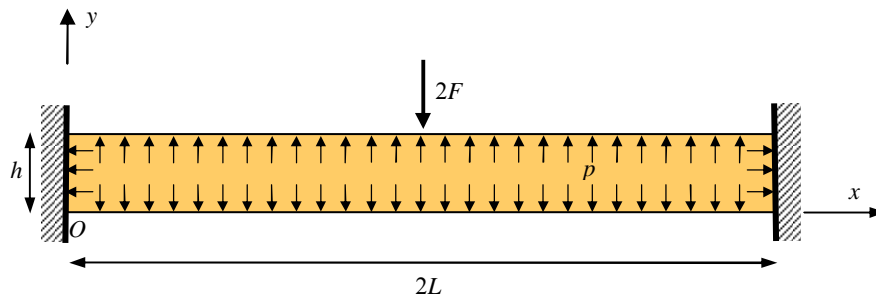


Figure 8: the built-in inflatable beam.

The inflated configuration together with the loaded one corresponding to a vertical displacement of the loaded point equal to 100 mm is showed in Figure 9.

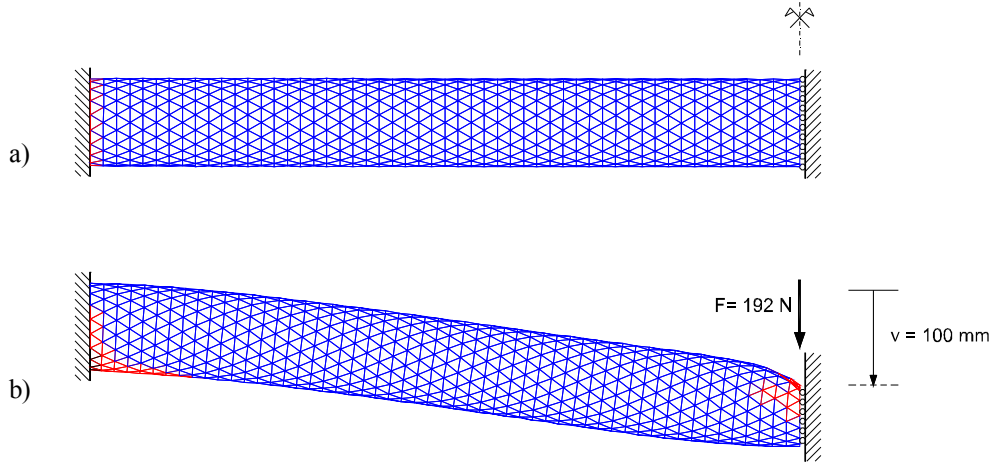


Figure 9: a) the inflated configuration; b) equilibrium configuration corresponding to $F = 192$ N (left half of the beam; red elements are in a wrinkled state; $p = 0.1$ N/mm², $E = 2500$ N/mm², $\nu = 0.3$, $t = 0.125$ mm)

Contrary to the simply-supported case examined in the preceding section, here a very small increase in the extension of the wrinkling regions (located under the point load and at the built-in ends) is observed as the force F grows.

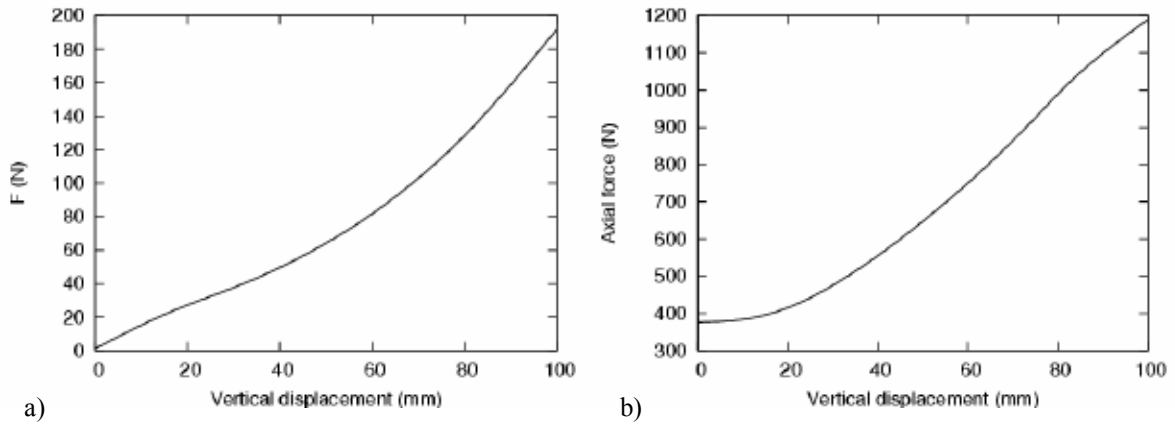


Figure 10: load-displacement curve (a) and axial force-displacement curve (b) for $p = 0.1$ N/mm² ($E = 2500$ N/mm², $\nu = 0.3$, $t = 0.125$ mm).

The strongly different behaviour of the built-in beam is highlighted in the load-displacement diagram showed in Figure 10a. The beam shows progressive stiffening as the vertical displacement of the loaded point increases and no softening phase is observed. This may be easily explained by considering the relevant increase in the tensile longitudinal force which takes place in this loading process (Figure 10b) and by remembering that the limit value for the bending moment which corresponds to the onset of wrinkling in the cross-section of the beam is proportional to the axial force.

The influence of the pressure level on the load-displacement response of the beam is showed in Figure 11. It is worth observing that, contrary to the previous case of a simply-supported beam, here an increase in the pressure does not always have a beneficial effect. In

effect, an optimum value for the pressure, whose value will depend upon the magnitude of the vertical displacement of the loaded point, seems to exist as shown in the figure.

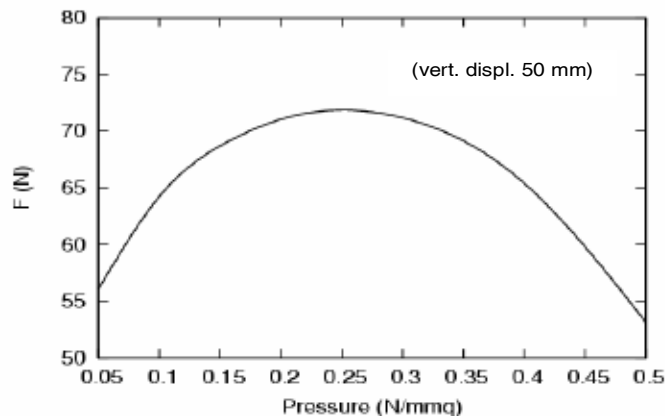


Figure 11: load vs. pressure diagram for vertical displacement of the loaded point equal to 50 mm ($p = 0.1 \text{ N/mm}^2$, $E = 2500 \text{ N/mm}^2$, $\nu = 0.3$, $t = 0.125 \text{ mm}$).

3 CONCLUSIONS

- Some features of the static behaviour of an inflated cylindrical beam subjected to a transversal concentrated load have been analyzed by means of a non-linear model which accounts for both large displacements and wrinkling of the membrane.
- The effects in terms of stress and of strain/displacements for increasing pressure and load levels have been examined for two beams: the first one simply-supported at its ends, the other built-in. The two beams showed completely different behaviours; moreover, in the case of the built-in beam, an optimum value for the pressure seems to exist for imposed load or displacement.

REFERENCES

- [1] R. Barsotti and S.S. Ligarò, "Equilibrium shapes of inflated elastic membranes", in *Proc Int. Conf. on Textile Composites and Inflatable Structures IV - STRUCTURAL MEMBRANES*, Stuttgart (Germany) (2009).
- [2] W.G. Davids, H. Zhang, A.W. Turner and M.L. Peterson, "Beam Finite-Element Analysis of Pressurized Fabric Tubes", *Journal of Struct. Eng.*, **133** (7), 990-998 (2007).
- [3] A. Le Van and C. Wielgosz, "Bending and buckling of inflatable beams: some new theoretical results", *Thin-Walled Structures*, **43**, 1166-1187 (2005).
- [4] C. Wielgosz and J.C. Thomas, "An inflatable fabric beam finite element", *Comm. In Num. Methods in Eng.*, **19**, 307-312 (2003).